EFFECTS OF TWO VIBRATION-DISSOCIATION COUPLING MODELS ON NONEQUILIBRIUM HYPERSONIC FLOW OF NITROGEN OVER A WEDGE

by Fred R. DeJarnette

Langley Research Center
Langley Station, Hampton, Va.

NATIONAL AERONAUTICS AND SPACE ADMINISTRATION • WASHINGTON, D. C. • AUGUST 1966

NASA TN D-3521

EFFECTS OF TWO VIBRATION-DISSOCIATION COUPLING MODELS ON NONEQUILIBRIUM HYPERSONIC FLOW OF NITROGEN OVER A WEDGE

By Fred R. DeJarnette

Langley Research Center
Langley Station, Hampton, Va.

NATIONAL AERONAUTICS AND SPACE ADMINISTRATION

For sale by the Clearinghouse for Federal Scientific and Technical Information
Springfield, Virginia 22151 – Price $2.00

EFFECTS OF TWO VIBRATION-DISSOCIATION COUPLING MODELS ON NONEQUILIBRIUM HYPERSONIC FLOW OF NITROGEN OVER A WEDGE

By Fred R. DeJarnette
Langley Research Center

SUMMARY

The effects of the coupled vibration-dissociation (CVD) and coupled vibration-dissociation-vibration (CVDV) models on the inviscid, nonequilibrium flow over a wedge have been compared with the flow fields with no coupling (UVD model). The numerical method used for the flow-field computations makes use of Lax's finite-difference method but employs a modified-difference scheme on the wedge surface. Distributions of flow properties along and normal to the wedge surface are presented for the flow of nitrogen for free-stream Mach numbers of 15.25 and 23.76 past wedges with attached shock waves and wedge half-angles close to 43°.

At the lower Mach number of 15.25, where dissociation is small, the CVD and CVDV models gave identical results. However, the UVD model predicted a much larger degree of dissociation near the tip of the wedge than the CVD and CVDV models.

At the higher Mach number of 23.76, where dissociation is appreciable, large differences were observed between all three coupling models. The CVD model was found to have a dissociation overshoot in addition to the vibrational overshoot, whereas the CVDV model eliminated both of these overshoots. It was further found that the thickness of the shock layer is largest for the CVDV model and smallest for the UVD model.

As a result of the present investigation, it is concluded that the vibration-dissociation coupling does have a significant effect on the flow fields past finite bodies at the higher Mach numbers. Even for the Mach numbers where dissociation is small, the effect of the coupling mechanism on the degree of dissociation is appreciable.

INTRODUCTION

A considerable effort is currently being devoted to the determination of flow fields surrounding reentry vehicles traveling at velocities and altitudes where the gas in the flow field deviates significantly from a perfect gas and where nonequilibrium real-gas effects must be considered. In addition to the usual nonequilibrium vibrations and

dissociation associated with diatomic molecules, the coupling mechanism between the vibrational excitation and molecular dissociation has been shown to have a significant effect on the flow properties (refs. 1 and 2). Several coupling models have been developed (refs. 1 to 5) and used in the computation of nonequilibrium flow fields (refs. 1 to 13). The present paper examines the effect of two coupling models (compared with the uncoupled model) on the steady, inviscid flow of nitrogen past wedges.

Hammerling, Teare, and Kivel (ref. 1) developed a coupled vibration-dissociation (CVD) model which accounts for the vibrational nonequilibrium effects on the rate of dissociation. However, the normal shock-wave flow fields computed in references 6 and 7 showed that, at the higher shock strengths, the vibrational temperature overshoots the translational temperature. This phenomenon has been questioned on physical grounds in reference 14 and is no longer thought to be realistic. The main objection to the CVD model is that it does not account for the drain on vibrational energy due to the dissociation process. This CVD coupling was modified by Treanor and Marrone (ref. 2), and independently by Heims (ref. 3), to include the converse effects of dissociation on vibrational relaxation. The coupled vibration-dissociation-vibration (CVDV) model eliminates the vibrational overshoot observed in the CVD model.

Both the CVD and CVDV models contain two important assumptions:

(1) The relaxation of the vibrational degree of freedom to the final Boltzmann distribution at the equilibrium temperature is assumed to occur through a series of Boltzmann distributions.

(2) Dissociation can occur with equal probability from any vibrational level in a sufficiently energetic collision.

In reference 4 Marrone and Treanor modified assumption (2) so that dissociation could occur preferentially from the higher vibrational levels, and Marrone (ref. 11) compared the preferential model with the CVDV model for both normal and bow shock waves. A still more elaborate method was recently introduced by Treanor (ref. 5) for coupling the vibrations and dissociation by using non-Boltzmann distributions and different vibration and dissociation rates for the individual vibrational levels. This model also accounts for the coupling between recombination and vibrational relaxation, which is important in expanding flows. Although these two latter modifications are more realistic, their application to flow fields (other than one-dimensional problems) is quite tedious.

The purpose of the present paper is to compare the CVD and CVDV models with the uncoupled model (UVD) for the nonequilibrium flow of nitrogen past thick wedges with an attached shock wave. Although the CVD and CVDV models may oversimplify the actual coupling mechanism, they should be useful for assessing the importance of the nonequilibrium coupling effects on finite-body flow fields.

SYMBOLS

$[A_j]$	concentration of jth species, moles per cc
D	dissociation energy per molecule
$E(T,T_v)$	average value of energy lost from vibration due to dissociation (per unit mass)
E_v	vibrational energy per unit mass
$E_{v,e}$	equilibrium vibrational energy per unit mass
f	vibration-dissociation coupling factor defined by equation (26)
G(T)	average energy gained by vibration due to recombination (per unit mass)
H	static enthalpy per unit mass
H_t	total enthalpy per unit mass
h	Planck's constant
K_e	equilibrium constant for vibrational equilibrium
k_f	specific forward reaction-rate constant
k_r	specific reverse reaction-rate constant
l	length scale
M	locally frozen Mach number
m_j	mass of a molecule of jth species
$[N_2]$	concentration of nitrogen, moles per cc
n	number of vibrational energy levels included in dissociation energy
P	pressure, atm (unless otherwise noted)

Q	partition function
R	universal gas constant
T	translational temperature, ^{o}K
T_m	parameter defined by equation (27), ^{o}K
T_v	vibrational temperature, ^{o}K
t	time, sec
u,v	velocity components in x and y directions, respectively
V	velocity magnitude
W_j	molecular weight of jth species
x,y	coordinates along and normal to wedge surface, respectively
α	atom mass fraction, ρ_A/ρ
γ	locally frozen ratio of specific heats
Γ	rate of dissociation, $\frac{d\alpha}{dt}$
θ	wedge half-angle
$\Theta_D,\Theta_R,\Theta_v$	characteristic dissociational, rotational, and vibrational temperatures, respectively, ^{o}K
Λ	vibrational energy rate, $\frac{dE_v}{dt}$
ν	vibrational frequency
ρ	mass density
ρ_D	dissociation density function given by equation (23)

τ vibrational relaxation time, sec

ψ constant defined by equation (10)

Subscripts:

e equilibrium conditions

$e\ell$ electronic

f forward or dissociation reaction

j species
for general case: A or A_2
for specific case of nitrogen: N or N_2

r recombination or reverse reaction

vib eq vibrational equilibrium

∞ undisturbed free-stream conditions

Barred quantities are dimensionless (see eq. (7)); unbarred quantities are dimensional.

Abbreviations:

CVD coupling effect of vibration on dissociation

CVDV coupling effects of vibration on dissociation and dissociation on vibration

UVD uncoupled vibration and dissociation

ANALYSIS

The problem studied in this investigation is the effect of the CVD and CVDV coupling models on the steady, inviscid, hypersonic flow of nitrogen past thick wedges with an attached shock wave. A diatomic gas subject to harmonic vibrations, dissociation and recombination is considered. Translation and molecular rotation modes are

assumed to be fully excited, whereas the electronic internal energy and ionization are neglected. For more detail concerning the gas model, see references 1, 2, 3, and 15.

The numerical method used for the flow-field solution replaces the governing partial-differential equations with finite-difference equations. (See refs. 15, 16, and 17.) Then, with known flow properties along an initial data line near the tip of the wedge, the downstream flow field is computed by marching forward in the streamwise direction. This numerical technique is restricted to hyperbolic equations; hence, the steady-state flow field being computed must remain supersonic.

Basic Equations

The flow geometry and coordinate system are illustrated in the following sketch for a wedge. For this body-oriented coordinate system, x is measured along the surface of the wedge, y is normal to the surface, and the velocity components in these respective directions are u and v. The basic flow and rate equations (specialized for a wedge) are written in conservation (or divergence) form as (ref. 15) –

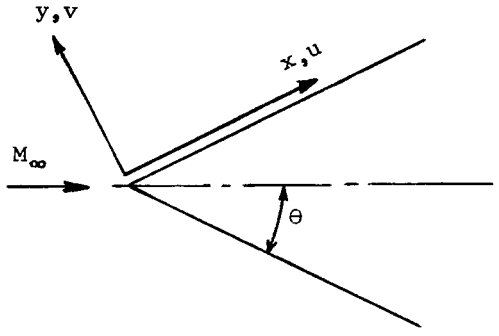

Continuity:

$$\frac{\partial(\bar{\rho}\bar{u})}{\partial\bar{x}} + \frac{\partial(\bar{\rho}\bar{v})}{\partial\bar{y}} = 0 \tag{1}$$

x-momentum:

$$\frac{\partial\left(\bar{p} + \bar{\rho}\bar{u}^2\right)}{\partial\bar{x}} + \frac{\partial(\bar{\rho}\bar{u}\bar{v})}{\partial\bar{y}} = 0 \tag{2}$$

y-momentum:

$$\frac{\partial(\bar{\rho}\bar{u}\bar{v})}{\partial\bar{x}} + \frac{\partial\left(\bar{p} + \bar{\rho}\bar{v}^2\right)}{\partial\bar{y}} = 0 \tag{3}$$

Vibrational energy rate:

$$\frac{\partial\left(\bar{\rho}\bar{u}\bar{E}_v\right)}{\partial\bar{x}} + \frac{\partial\left(\bar{\rho}\bar{v}\bar{E}_v\right)}{\partial\bar{y}} - \frac{\bar{\rho}\,l\,W_{A_2}\Lambda}{V_\infty T_\infty R} = 0 \tag{4}$$

Rate of dissociation:

$$\frac{\partial(\bar{\rho}\bar{u}\alpha)}{\partial\bar{x}} + \frac{\partial(\bar{\rho}\bar{v}\alpha)}{\partial\bar{y}} - \frac{\bar{\rho}\,l\Gamma}{V_\infty} = 0 \tag{5}$$

Energy:

$$\overline{H} + \frac{\overline{u}^2 + \overline{v}^2}{2} = \overline{H}_t = \text{Constant} \tag{6}$$

The nondimensional vibrational energy is $\overline{E}_v$, α is the atom mass fraction (ρ_A/ρ), Λ is the dimensional vibration rate (dE_v/dt), and Γ is the dimensional dissociation rate $(d\alpha/dt)$. All quantities have been nondimensionalized as follows (barred quantities are nondimensional):

$$\left.\begin{aligned} \overline{u},\overline{v} &= \frac{u,v}{V_\infty} & \overline{P} &= \frac{P}{\rho_\infty V_\infty{}^2} & \overline{\rho} &= \frac{\rho}{\rho_\infty} \\ \overline{T} &= \frac{T}{T_\infty} & \overline{H} &= \frac{H}{V_\infty{}^2} & \overline{x},\overline{y} &= \frac{x,y}{l} \\ \overline{E}_v &= \frac{E_v W_{A_2}}{RT_\infty} & \overline{\Theta}_D,\overline{\Theta}_R,\overline{\Theta}_v &= \frac{\Theta_D,\Theta_R,\Theta_v}{T_\infty} \end{aligned}\right\} \tag{7}$$

The equations for enthalpy and state (see refs. 15 and 16) are –

Enthalpy:

$$\overline{H} = \psi\left[\left(\frac{7 + 3\alpha}{2}\right)\overline{T} + (1 - \alpha)\overline{E}_v + \alpha\overline{\Theta}_D\right] \tag{8}$$

State:

$$\overline{P} = \overline{\rho}\overline{T}(1 + \alpha)\psi \tag{9}$$

where

$$\psi \equiv \frac{RT_\infty}{W_{A_2} V_\infty{}^2} = \left[\gamma_\infty\left(1 + \alpha_\infty\right)M_\infty{}^2\right]^{-1} \tag{10}$$

The locally frozen ratio of specific heats is

$$\gamma = \frac{7 + 3\alpha}{5 + \alpha} \tag{11}$$

and the locally frozen Mach number is

$$M = \left(\frac{u^2 + v^2}{\gamma P/\rho}\right)^{1/2} = \left[\frac{\left(u^2 + v^2\right)W_{A_2}}{\gamma(1 + \alpha)RT}\right]^{1/2} \tag{12}$$

The coupling models affect the vibrational and dissociational rates, Λ and Γ. The characteristic dissociation temperature for nitrogen, Θ_D, is $113{,}240^\circ$ K.

Vibrational Rate

A linear harmonic oscillator model is assumed for the diatomic vibrations. The vibrational relaxation, neglecting the dissociation coupling effect, is from reference 18

$$\frac{dE_v}{dt} = \Lambda = \frac{E_{v,e} - E_v}{\tau} \tag{13}$$

where the equilibrium vibrational energy at the local translational temperature is

$$E_{v,e} = \frac{R\Theta_v}{W_{A_2}\left(e^{\Theta_v/T} - 1\right)} \tag{14}$$

The characteristic vibrational temperature Θ_v for nitrogen is given by reference 19 as 3396° K. Reference 2, where numerical fits were made to Blackman's data (ref. 20), gives the vibrational relaxation time τ in sec for nitrogen as

$$\tau = \left(1.1 \times 10^{-11}\right)\frac{T^{1/2}}{P}\exp\left(\frac{154}{T^{1/3}}\right) \tag{15}$$

Equation (13) represents the vibrational energy rate for both the UVD and CVD models. However, it must be modified by an expression which accounts for the coupling effect of dissociation on vibrational relaxation when considering the CVDV model.

Dissociation Rate

For the dissociation of nitrogen, reference 2 gives the following chemical reactions:

$$N_2 + N \underset{k_{r_1}}{\overset{k_{f_1}}{\rightleftharpoons}} 2N + N \tag{16}$$

$$N_2 + N_2 \underset{k_{r_2}}{\overset{k_{f_2}}{\rightleftharpoons}} 2N + N_2 \tag{17}$$

For nitrogen, the experimental forward reaction-rate constants are not known; however, reference 2 gives the reverse reaction-rate constants as

$$k_{r_1} = (3.33)10^{21}T^{-1.5}\ \frac{cm^6}{mole^2\text{-}sec} \tag{18}$$

$$k_{r_2} = (3.33)10^{19}T^{-1.5}\ \frac{cm^6}{mole^2\text{-}sec} \tag{19}$$

The net rate of production of the atom mass fraction for the reactions given by equations (16) and (17) is (ref. 15)

$$\frac{d\alpha}{dt} = \Gamma = \frac{2k_{r_1}\rho\alpha}{W_N^2}\left[\frac{k_{f_1}}{k_{r_1}}\frac{(1-\alpha)W_{N_2}}{4} - \rho\alpha^2\right] + \frac{k_{r_2}\rho(1-\alpha)}{W_N^2}\left[\frac{k_{f_2}}{k_{r_2}}\frac{(1-\alpha)W_{N_2}}{4} - \rho\alpha^2\right] \tag{20}$$

Equation (20) gives the dissociation rate once appropriate expressions for the forward reaction-rate constants have been determined. These constants are in turn dependent on the particular coupling considered (UVD, CVD, or CVDV).

When the vibrational energy is in equilibrium with the translational mode, the forward and reverse reaction-rate constants are related through the equilibrium constant

$$K_e = \frac{(k_f)_{\text{vib eq}}}{k_r} \tag{21}$$

(It is assumed that vibrational nonequilibrium does not affect k_r.) The equilibrium constant K_e can be calculated from molecular properties by the use of quantum statistical mechanics. For the reactions given by equations (16) and (17), the equilibrium constant is (ref. 21)

$$K_e = \frac{4\rho_D e^{-\Theta_D/T}}{W_{N_2}} \tag{22}$$

where

$$\rho_D = \frac{m_N(\pi m_N kT)^{3/2}}{2h^3}\left(\frac{2\Theta_R}{T}\right)\left(1 - e^{-\Theta_v/T}\right)\left(\frac{Q_{el,N}^2}{Q_{el,N_2}}\right) \tag{23}$$

m_N mass of a molecule of atomic nitrogen

h Planck's constant

k Boltzmann's constant

Θ_R characteristic rotational temperature, 2.847° K for nitrogen

Q_{el} electronic partition function

As shown in appendix B of reference 19, the electronic partition functions for nitrogen vary less than 5 percent for $1500^{\circ}\ K < T < 8000^{\circ}\ K$. Therefore, average values over this temperature range are just the degeneracies of the ground states

$$Q_{el,N_2} = 1 \qquad Q_{el,N} = 4$$

Uncoupled Vibration-Dissociation (UVD) Model

In the earlier analyses of nonequilibrium flows the vibrational relaxation and molecular dissociation were not coupled. The measured reaction-rate constant was used as the actual reaction-rate constant, and the opposing reaction-rate constant was determined through the equilibrium constant. Thus the UVD model sets

$$k_f = (k_f)_{vib\ eq}$$

and the forward reaction-rate constants for the UVD model are (from eq. (21)):

$$k_{f_1} = K_e k_{r_1} \tag{24}$$

$$k_{f_2} = K_e k_{r_2} \tag{25}$$

The vibrational rate equation for the UVD model is given by equation (13).

Coupled Vibration-Dissociation (CVD) Model

The use of the equilibrium constant to relate the forward and reverse reaction-rate constants (eq. (21)) is justified only when vibrational equilibrium exists. Hammerling, Teare, and Kivel (ref. 1) developed the CVD coupling to account for the effect of vibrational relaxation on molecular dissociation. By using the harmonic-oscillator calculations of Montroll and Shuler (ref. 22), the ratio of the dissociation-rate constant to the value with vibrational equilibrium was found to be

$$f \equiv \frac{k_f}{(k_f)_{vib\ eq}} = \frac{1}{n}\left(\frac{1 - e^{-n\Theta_v/T_m}}{e^{\Theta_v/T_m} - 1}\right)\frac{\left(e^{\Theta_v/T_v} - 1\right)}{\left(e^{\Theta_v/T} - 1\right)} \tag{26}$$

where

$$\frac{1}{T_m} = \frac{1}{T_v} - \frac{1}{T} \tag{27}$$

$$E_v = \frac{R\Theta_v}{W_{N_2}\left(e^{\Theta_v/T_v} - 1\right)} \tag{28}$$

and n is the smallest integer greater than $D/h\nu$, that is, integral number of vibrational levels up to the dissociation cut-off, which for nitrogen is 34.

Thus the nitrogen reverse-rate constants for the CVD model are given by equations (18) and (19), whereas the forward reaction-rate constants are

$$k_{f_1} = f\left(k_{f_1}\right)_{\text{vib eq}} = f\, k_{r_1}\left(K_e\right) \tag{29}$$

$$k_{f_2} = f\left(k_{f_2}\right)_{\text{vib eq}} = f\, k_{r_2}\left(K_e\right) \tag{30}$$

The effect of the coupling given by equation (26) is to slow down the dissociation rates in the region where $E_v < E_{v,e}$ since $0 < f < 1$. However, in the region of the vibrational overshoot $\left(T_v > T\right)$, which occurs with the CVD model, the dissociational rates are increased because $f > 1$ for $T_v > T$.

Coupled Vibration-Dissociation-Vibration (CVDV) Model

The CVD model does not include the converse effect of molecular dissociation on vibrational relaxation. To account for this additional effect in the coupling of vibrations and dissociation, Treanor and Marrone (ref. 2) modified the vibrational-energy-rate equation given by equation (13) to the form

$$\frac{dE_v}{dt} = \frac{E_{v,e} - E_v}{\tau} - \frac{E\left(T,T_v\right)}{\left[A_2\right]}\left(\frac{d\left[A_2\right]}{dt}\right)_f + \frac{G(T)}{\left[A_2\right]}\left(\frac{d\left[A_2\right]}{dt}\right)_r + \frac{E_v}{\left[A_2\right]}\left[\left(\frac{d\left[A_2\right]}{dt}\right)_f - \left(\frac{d\left[A_2\right]}{dt}\right)_r\right] \tag{31}$$

where $\left[A_2\right]$ is the concentration (moles/cc) of the diatomic molecules considered, and the subscripts f and r refer to the forward (dissociative) process and reverse (recombination) process. The $E\left(T,T_v\right)$ term is the average value of the energy lost from vibration due to dissociation, G(T) is the average energy gained by vibration due to recombination, and the last term in equation (31) accounts for the change in the number of oscillators during dissociation. Note that both $\left(\frac{d\left[A_2\right]}{dt}\right)_f$ and $\left(\frac{d\left[A_2\right]}{dt}\right)_r$ are used as positive quantities in equation (31).

Using the same assumptions as for the CVD model, Treanor and Marrone obtained

$$E\left(T,T_v\right) = \frac{R\Theta_v}{\overline{W}_{N_2}}\left[\frac{1}{\left(e^{\Theta_v/T_m} - 1\right)} - \frac{n}{\left(e^{n\Theta_v/T_m} - 1\right)}\right] \tag{32}$$

and

$$G(T) = \frac{R\Theta_v}{W_{N_2}}\left(\frac{n - 1}{2}\right) \tag{33}$$

Therefore, the vibrational rate for the CVDV model is

$$\frac{dE_v}{dt} = \Lambda$$

$$= \frac{E_{v,e} - E_v}{\tau} - \left[\frac{R\Theta_v}{W_{N_2}}\left(\frac{1}{e^{\Theta_v/T_m} - 1} - \frac{n}{e^{n\Theta_v/T_m} - 1}\right) - E_v\right]\frac{1}{[N_2]}\left(\frac{d[N_2]}{dt}\right)_f + \left[\frac{R\Theta_v}{W_{N_2}}\left(\frac{n - 1}{2}\right) - E_v\right]\frac{1}{[N_2]}\left(\frac{d[N_2]}{dt}\right)_r \tag{34}$$

The same reaction-rate constants are used for the CVDV model as for the CVD model. For the reactions given by equations (16) and (17),

$$\frac{1}{[N_2]}\left(\frac{d[N_2]}{dt}\right)_f = \frac{\rho}{W_{N_2}}\left[2k_{f_1}\alpha + k_{f_2}(1 - \alpha)\right] \tag{35}$$

$$\frac{1}{[N_2]}\left(\frac{d[N_2]}{dt}\right)_r = \frac{4\rho^2\alpha^2}{W_{N_2}^2(1 - \alpha)}\left[2k_{r_1}\alpha + k_{r_2}(1 - \alpha)\right] \tag{36}$$

At relatively low shock strengths, where the degree of dissociation is small, the CVD and CVDV models give identical results. At higher shock strengths, the CVDV model eliminates the vibrational temperature overshoot observed in the CVD model. The CVDV model in turn predicts a slower rate of dissociation since $T_v < T$ (and thus $f < 1$) throughout the entire relaxation process.

Method for Numerical Computations

The numerical method used for the flow-field computations is described in reference 16. Basically, the method replaces the partial-differential equations with finite-difference equations, by using the difference scheme of Lax (ref. 17) along with a modified-difference method for the boundary points. As a consequence of Lax's difference scheme an artificial viscosity is implicitly introduced and allows the computations to proceed downstream of an initial data line as if no shock wave were present at all. The shock wave appears in the solution, however, smeared over several mesh spaces while accurately giving the proper jump conditions across the shock. Approximate flow properties on the initial data line, which is near the tip of the wedge and normal to the surface, are determined from the wedge-tip gradients given in appendix C of reference 16.

Since the system of equations being solved is hyperbolic, the ratio of the mesh spacing in the x-direction to the mesh spacing in the y-direction is limited by the hyperbolic stability criterion. The free stream as well as the shock layer must be considered in determining the stability criterion because the computations carry through the shock wave. For all the examples given here, the free-stream stability criterion was more stringent than that of the shock layer since the free-stream velocity is inclined at the wedge half-angle θ to the coordinate system. (See ref. 16 for the details.)

RESULTS AND DISCUSSION

References 1, 2, and 12 show the effect of the CVD and CVDV couplings on the one-dimensional flow downstream of normal shock waves. However, these effects have not been investigated for flow fields past bodies. Therefore, the following cases were computed to determine the differences between the UVD, CVD, and CVDV gas models for flow over wedges. In each case the shock-wave angle at the tip of the wedge was chosen to be 59°. The Mach numbers were chosen so that the shock strengths at the wedge tip would be the same as those for the normal shock solutions computed in reference 2.

Case I

Gas = Nitrogen	$M_\infty = 15.24987$	$\theta = 43.066^{\circ}$
$T_\infty = 285^{\circ}$ K	$P_\infty = 1$ mm Hg	$E_{V,\infty} = 0$
$\alpha_\infty = 0$		

Case II

Gas = Nitrogen	$M_\infty = 23.75726$	$\theta = 43.319^{\circ}$
$T_\infty = 285^{\circ}$ K	$P_\infty = 1$ mm Hg	$E_{V,\infty} = 0$
$\alpha_\infty = 0$		

Figures 1 to 4 give the variation of $\overline{P}$, $\overline{T}$, $\overline{E}_V$, and α along the wedge surface for Case I ($M_\infty = 15.24987$). These results follow the trend shown in reference 16; and, to the scale of these figures, there is no difference between the CVD and CVDV models. The UVD model gives the same results as the CVD and CVDV models for $\overline{P}$, $\overline{T}$, and $\overline{E}_V$. However, figure 4 shows that the degree of dissociation is much larger for the UVD model than for the other two, particularly near the tip of the wedge. Due to the small magnitudes of α, these differences have very little effect on the other flow variables.

Figure 5 gives the pressure distribution along the wedge surface for Case II ($M_\infty = 23.75726$). In order to carry the solutions out to $x = 100$ cm, it was necessary to increase the mesh scale for $x > 2$ cm. After increasing the mesh scale, the behavior of the pressure was questionable, but still maintained a value close to that at $x = 2$ cm.

Therefore, the pressure curve in figure 5 was stopped at $x = 2$ cm. Although the pressure was questionable for $x > 2$ cm, the other properties should be accurate. The justification for this fact is that the comparisons given in references 16, 23, and 24 show that accurate surface properties can be obtained even where the pressure is not accurate.

Figures 6, 7, and 8 illustrate the large differences between the UVD, CVD, and CVDV models for $\overline{T}$, $\overline{E}_V$, and α. In addition to the vibrational overshoot for the CVD model (which can be deduced from fig. 7), figure 8 shows a dissociation overshoot ($\alpha > \alpha_e$) for the CVD model. This dissociation overshoot has not previously been reported in other flow-field computations. As a consequence of the vibrational and dissociational overshoots, the $\overline{T}$ and $\overline{E}_V$ curves for the CVD model exhibit "buckets" in their surface distribution. The CVDV model eliminates both of these overshoots. Figure 8 shows the same early increase in α for the UVD model as was found in Case I.

The profiles of the flow properties normal to the wedge surface at $x = 2$ cm are given in figures 9 to 12 for Case II. All these figures show that the shock layer is largest for the CVDV model and smallest for the UVD model.

The large effects produced by the coupling models in Case II can be explained by the coupling factor f given in equation (26). A study of the results obtained here revealed that the forward reaction rate dominated the reaction over the major portion of the flow field downstream of the tip of the wedge. The forward-rate constant was determined from

$$k_f = f(K_e)k_r$$

and for the UVD model $f \equiv 1$, whereas for the CVD and CVDV models

$$0 < f < 1 \quad \text{for} \quad E_V < E_{V,e}$$

$$f > 1 \quad \text{for} \quad E_V > E_{V,e}$$

This causes the CVDV model dissociation rate to be slower than for the UVD model since $E_V < E_{V,e}$ throughout the flow field. However, the CVD model has $E_V < E_{V,e}$ near the tip of the wedge, but the vibrational overshoot $(E_V > E_{V,e})$ makes $f > 1$ which in turn increases the dissociational rate over that predicted by the UVD model and leads to the dissociation overshoot observed for the CVD model.

It should be noted that, for the temperatures and pressures encountered in Case II, the effects of vibrational anharmonicity, electronic internal energy, and ionization are not necessarily small, although the present analysis does not consider these effects.

CONCLUDING REMARKS

The effects of the CVD and CVDV coupling models on the nonequilibrium flow of nitrogen past wedges have been compared with the uncoupled (UVD) model. Mach numbers of 15.25 and 23.76 were considered for wedges with half-angles near 43°.

At the lower Mach number of 15.25, where dissociation is small, the CVD and CVDV models gave identical results. However, the UVD model predicted a much larger degree of dissociation near the tip of the wedge than the CVD and CVDV models.

For the higher Mach number of 23.76, where dissociation is appreciable, large differences were observed between all three coupling models. The CVD model was found to have a dissociation overshoot in addition to the vibrational overshoot, whereas the CVDV model eliminated both of these overshoots. It was further found that the thickness of the shock layer is largest for the CVDV model and smallest for the UVD model.

As a result of the present investigation, it is concluded that the vibration-dissociation coupling does have a significant effect on the flow fields past finite bodies at the higher Mach numbers. Even for the Mach numbers where dissociation is small, the effect of the coupling mechanism on the degree of dissociation is appreciable.

Langley Research Center,
National Aeronautics and Space Administration,
Langley Station, Hampton, Va., April 6, 1966.

REFERENCES

1. Hammerling P.; Teare, J. D.; and Kivel, B.: Theory of Radiation from Luminous Shock Waves in Nitrogen. Phys. Fluids, vol. 2, no. 4, July-Aug. 1959, pp. 422-426.

2. Treanor, Charles E.; and Marrone, Paul V.: The Effect of Dissociation on the Rate of Vibrational Relaxation. Rept. No. QM-1626-A-4 (Contract No. DA-30-069-ORD-3443), Cornell Aeron. Lab., Inc., Feb. 1962.

3. Heims, S. P.: Moment Equations for Vibrational Relaxation Coupled With Dissociation. J. Chem. Phys., vol. 38, no. 3, Feb. 1, 1963, pp. 603-606.

4. Marrone, Paul V.; and Treanor, Charles E.: Chemical Relaxation With Preferential Dissociation from Excited Vibrational Levels. Rept. No. QM-1626-A-10 (Contract No. DA-30069-ORD-3443), Cornell Aeron. Lab., Inc., Feb. 1963.

5. Treanor, Charles E.: Coupling of Vibration and Dissociation in Gasdynamic Flows. Paper No. 65-29, Am. Inst. Aeron. Astronaut., Jan. 25-27, 1965.

6. Batchelder, R. A.: Normal Shock Waves in Air With Chemical and Vibrational Relaxation Effects Model – General. Rept. SM-37627, Missile and Space Systems Div., Douglas Aircraft Co., Inc., July 1960.

7. Hall, J. Gordon; Eschenroeder, Alan Q.; and Marrone, Paul V.: Inviscid Hypersonic Airflows With Coupled Nonequilibrium Processes. Rept. No. AF-1413-A-2(AFOSR 2072), Cornell Aeron. Lab., Inc., May 1962.

8. Allen, R. A.; Keck, J. C.; and Camm, J. C.: Non-Equilibrium Radiation From Shock Heated Nitrogen and a Determination of the Recombination Rate. Res. Rept. 110 (AFBSD-TR-61-20), Avco-Everett Res. Lab., June 1961.

9. Wurster, Walter H.; and Marrone, Paul V.: Study of Infrared Emission in Heated Air. Rept. No. QM-1373-A-4 (Contract DA-11-022-ORD-3130), Cornell Aeron. Lab., Inc., July 1961.

10. Wray, Kurt L.; and Teare, J. Derek: Shock-Tube Study of the Kinetics of Nitric Oxide at High Temperatures. J. Chem. Phys., vol. 36, no. 10, May 15, 1962, pp. 2582-2596.

11. Marrone, Paul V.: Inviscid, Nonequilibrium Flow Behind Bow and Normal Shock Waves, Part I. General Analysis and Numerical Examples. Rept. No. QM-1626-A-12(I) (Contract No. DA-30-069-ORD-3443), Cornell Aeron. Lab., Inc., May 1963.

12. Greenblatt, M.: The Coupling of Vibrational Relaxation and Dissociation. VKI-TN-19, Von Karman Inst. Fluid Dyn., 1964.

13. Bray, K. N. C.: Coupling Between Atomic Recombination and Vibrational Relaxation in Expanding Gas Flows. A.A.S.U. Rept. No. 260, Univ. of Southampton, Sept. 1964.

14. Bauer, S. H.; and Tsang, S. C.: Mechanisms for Vibrational Relaxation at High Temperatures. Phys. Fluids, vol. 6, no. 2, Feb. 1963, pp. 182-189.

15. DeJarnette, Fred R.: Numerical Solution of Inviscid Hypersonic Flows for Nonequilibrium Vibration and Dissociation Using an "Artificial Viscosity" Method. Ph. D. Thesis, Virginia Polytech. Inst., Mar. 1965.

16. DeJarnette, Fred R.: Application of Lax's Finite-Difference Method to Nonequilibrium Hypersonic Flow Problems. NASA TR R-234, 1966.

17. Lax, Peter D.: Weak Solutions of Nonlinear Hyperbolic Equations and Their Numerical Computation. Commun. Pure Appl. Math., vol. VII, no. 1, Feb. 1954, pp. 159-193.

18. Rossini, Frederick D., ed.: Thermodynamics and Physics of Matter. Vol. I of High Speed Aerodynamics and Jet Propulsion. Princeton Univ. Press, 1955.

19. Heims, Steve P.: Effects of Chemical Dissociation and Molecular Vibrations on Steady One-Dimensional Flow. NASA TN D-87, 1959.

20. Blackman, Vernon: Vibrational Relaxation in Oxygen and Nitrogen. J. Fluid. Mech., vol. 1, pt. 1., May 1956, pp. 61-85.

21. Freeman, N. C.: Dynamics of a Dissociating Gas – Part III. Non-Equilibrium Theory. Rept. 133, AGARD, North Atlantic Treaty Organization (Paris), July 1957.

22. Montroll, Elliott W.; and Shuler Kurt E.: Studies in Nonequilibrium Rate Processes. I. The Relaxation of a System of Harmonic Oscillators. J. Chem. Phys., vol. 26, no. 3, Mar. 1957, pp. 454-464.

23. South, Jerry C., Jr.: Application of the Method of Integral Relations to Supersonic Nonequilibrium Flow Past Wedges and Cones. NASA TR R-205, 1964.

24. Newman, Perry A.: A Modified Method of Integral Relations for Supersonic Nonequilibrium Flow Over a Wedge. NASA TN D-2654, 1965.

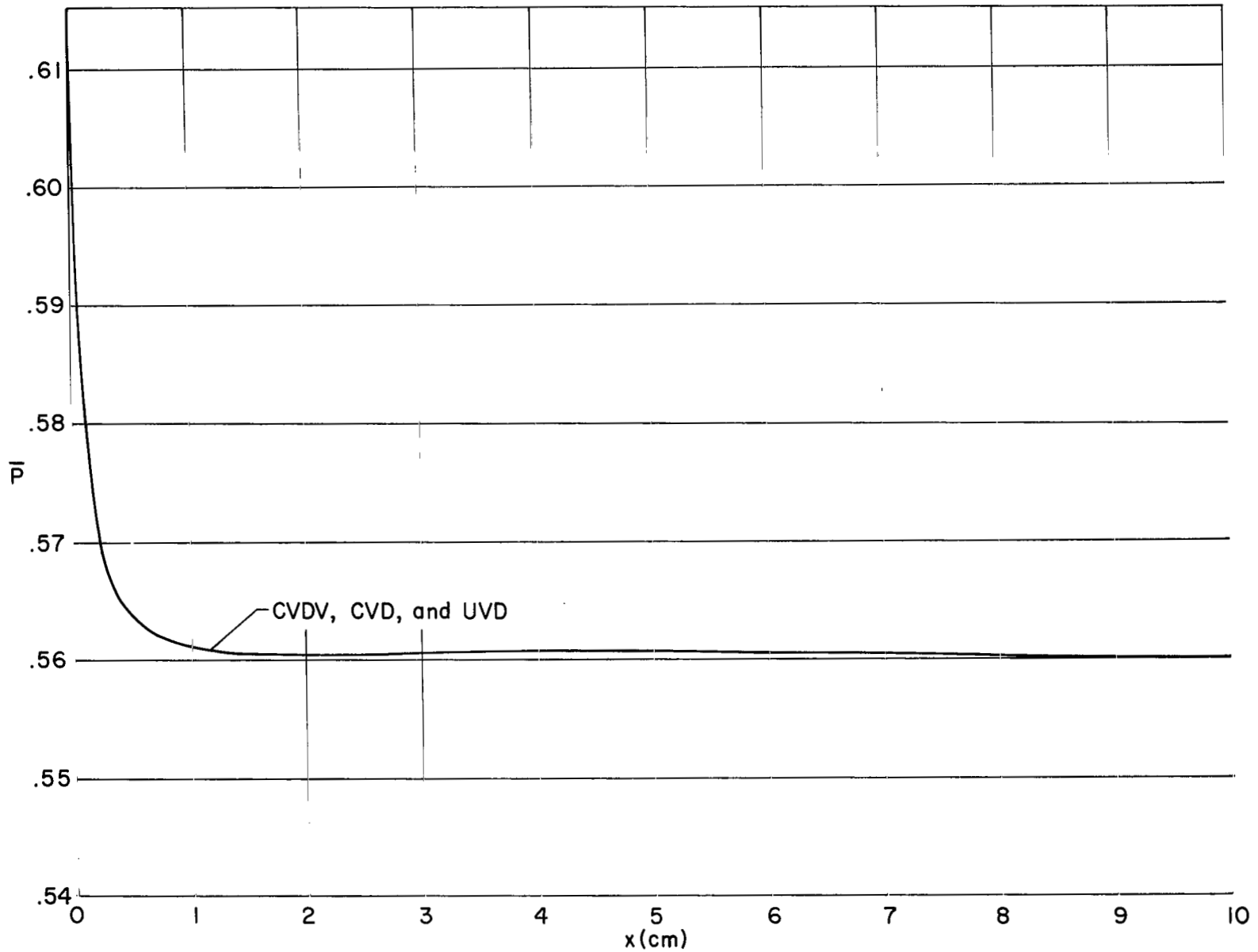

Figure 1.- Pressure along wedge surface for Case 1.

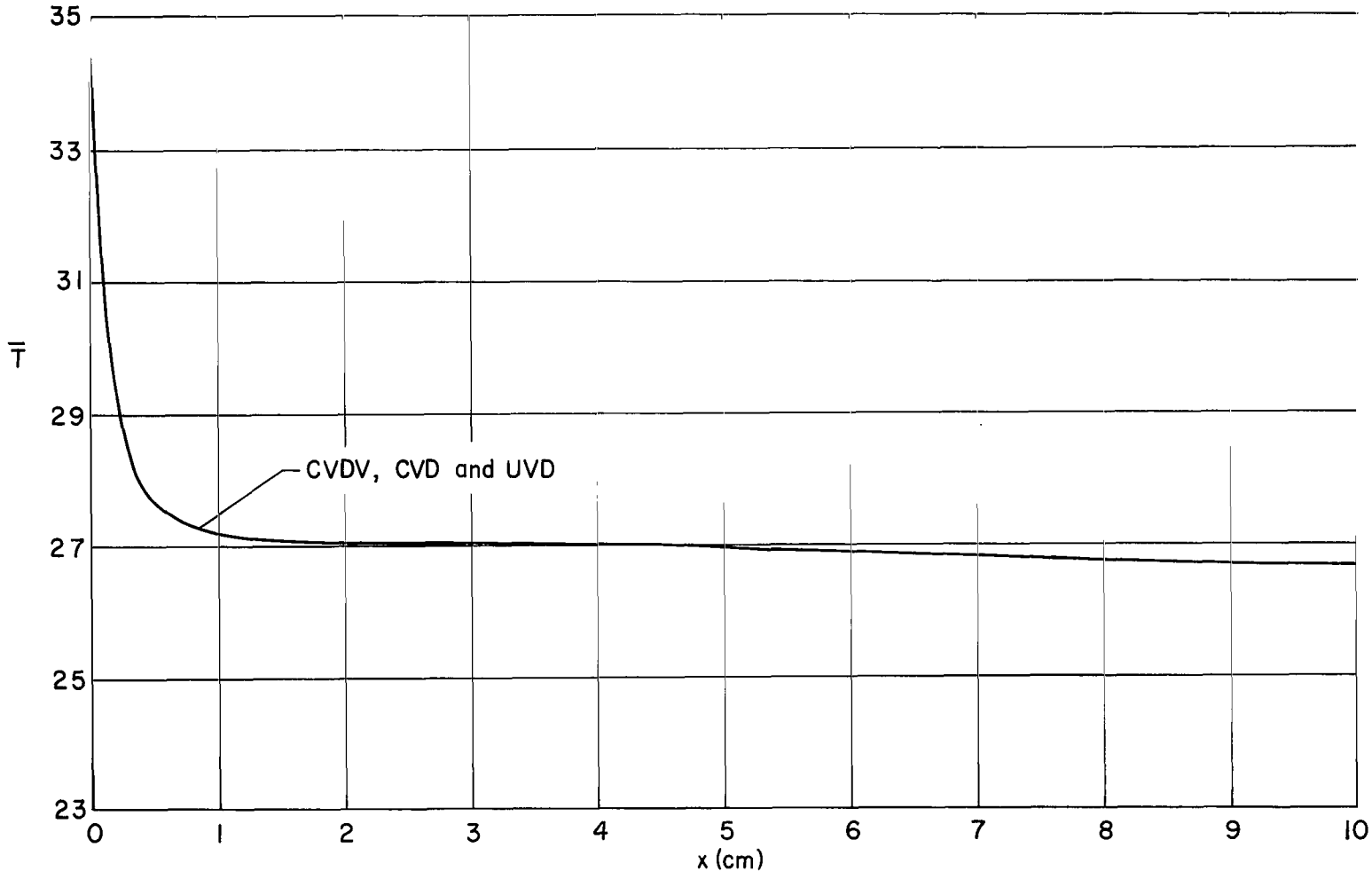

Figure 2.- Temperature along wedge surface for Case 1.

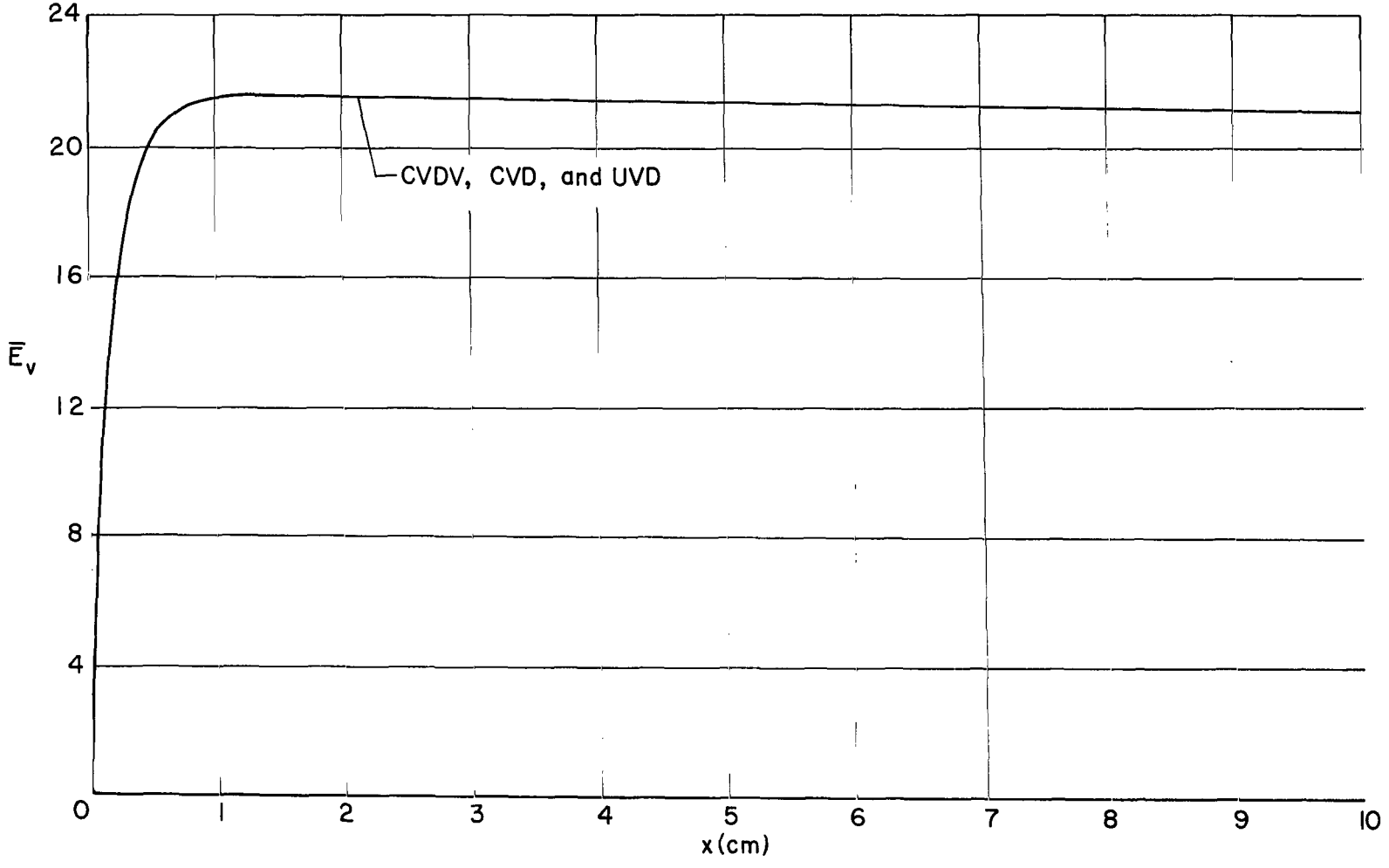

Figure 3.- Vibrational energy along wedge surface for Case I.

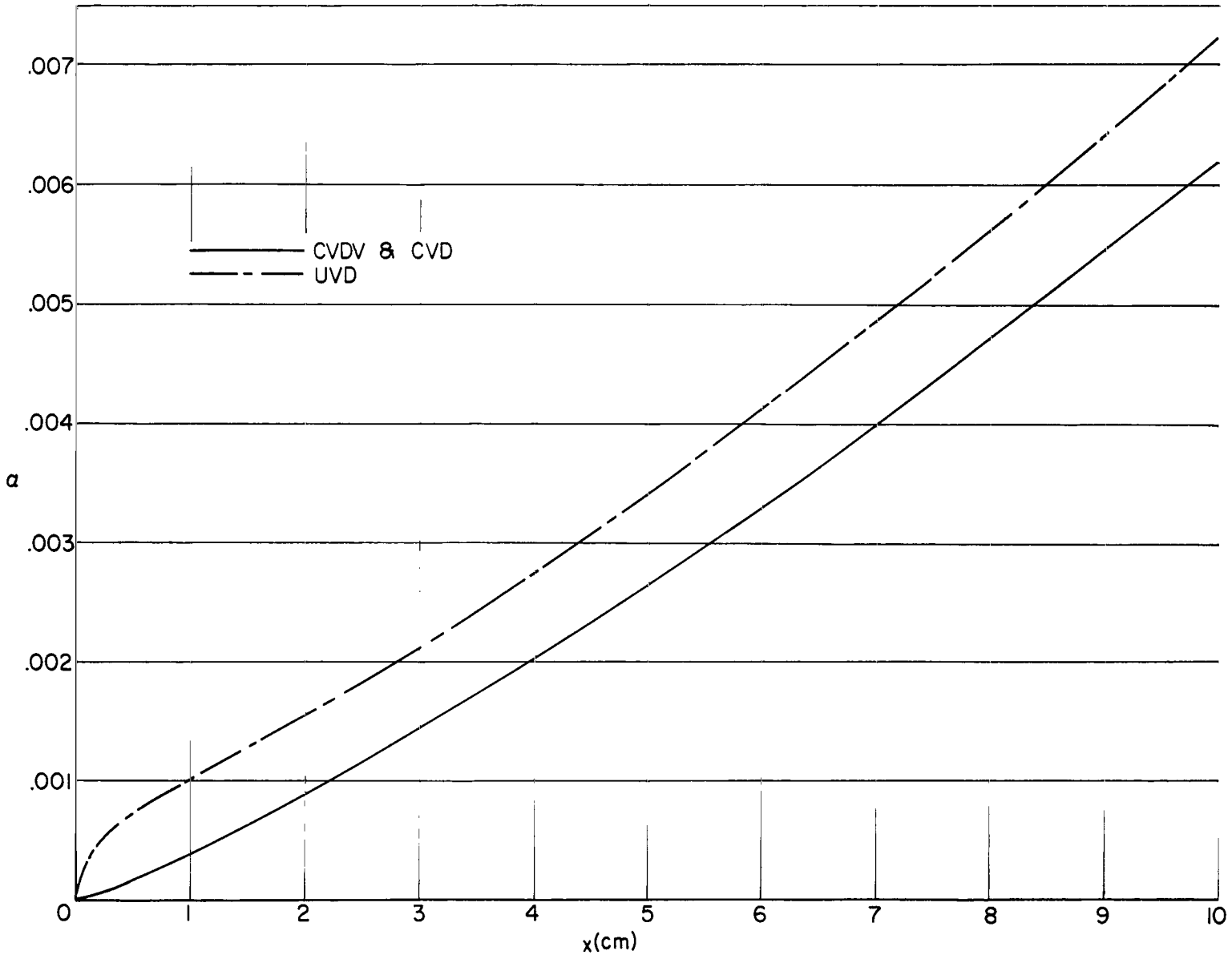

Figure 4.- Atom mass fraction along wedge surface for Case I.

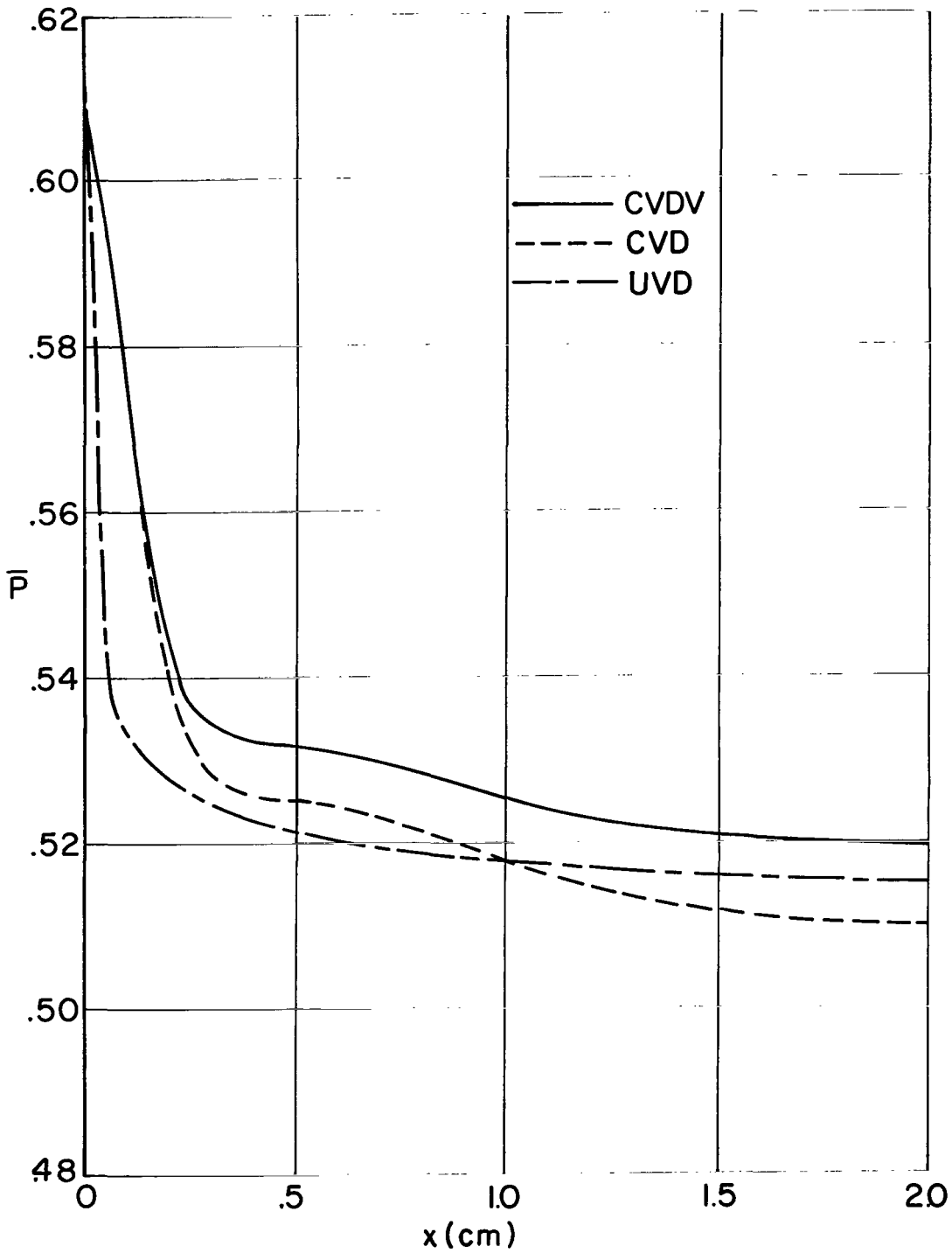

Figure 5.- Pressure along wedge surface for Case II.

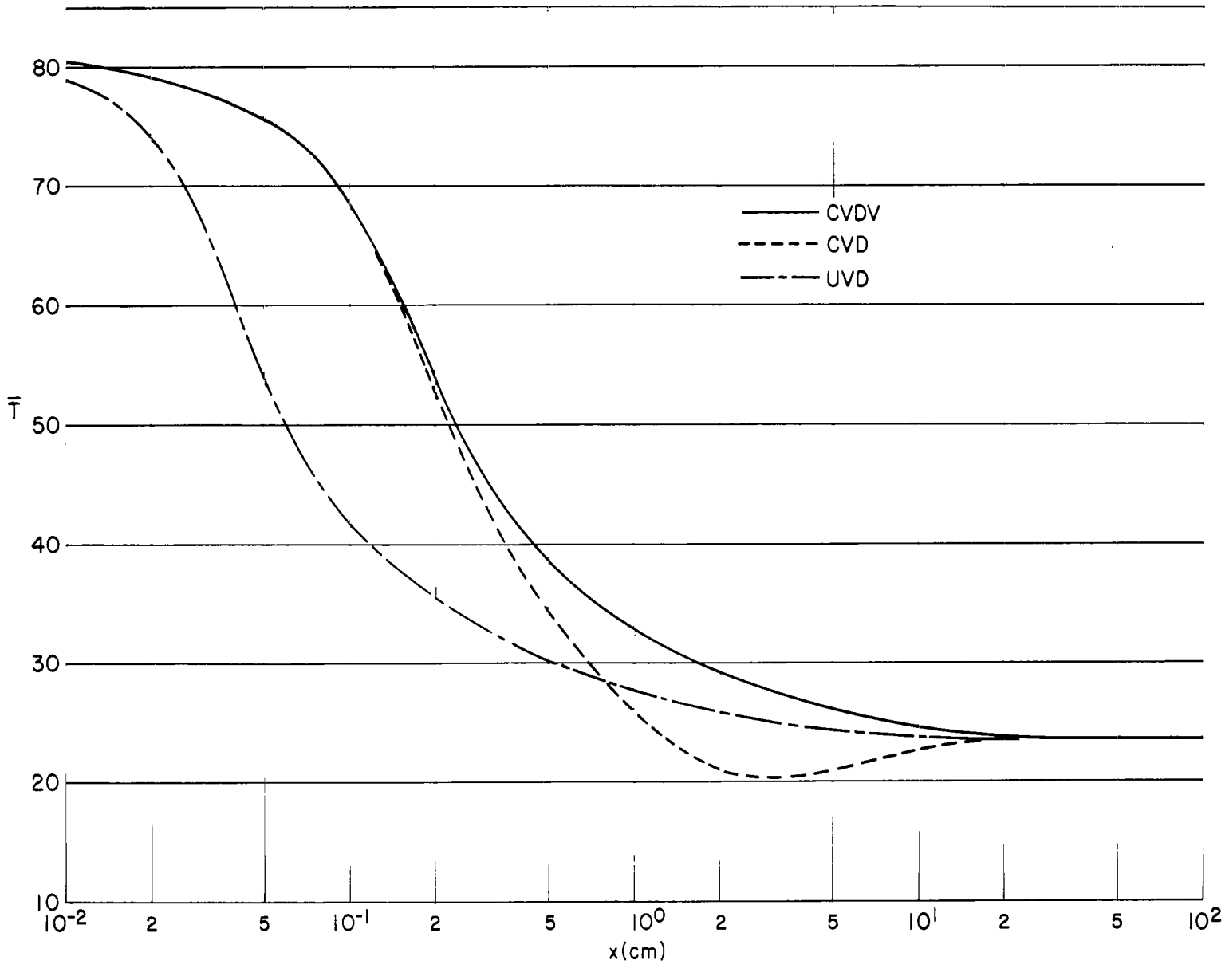

Figure 6.- Temperature along wedge surface for Case II.

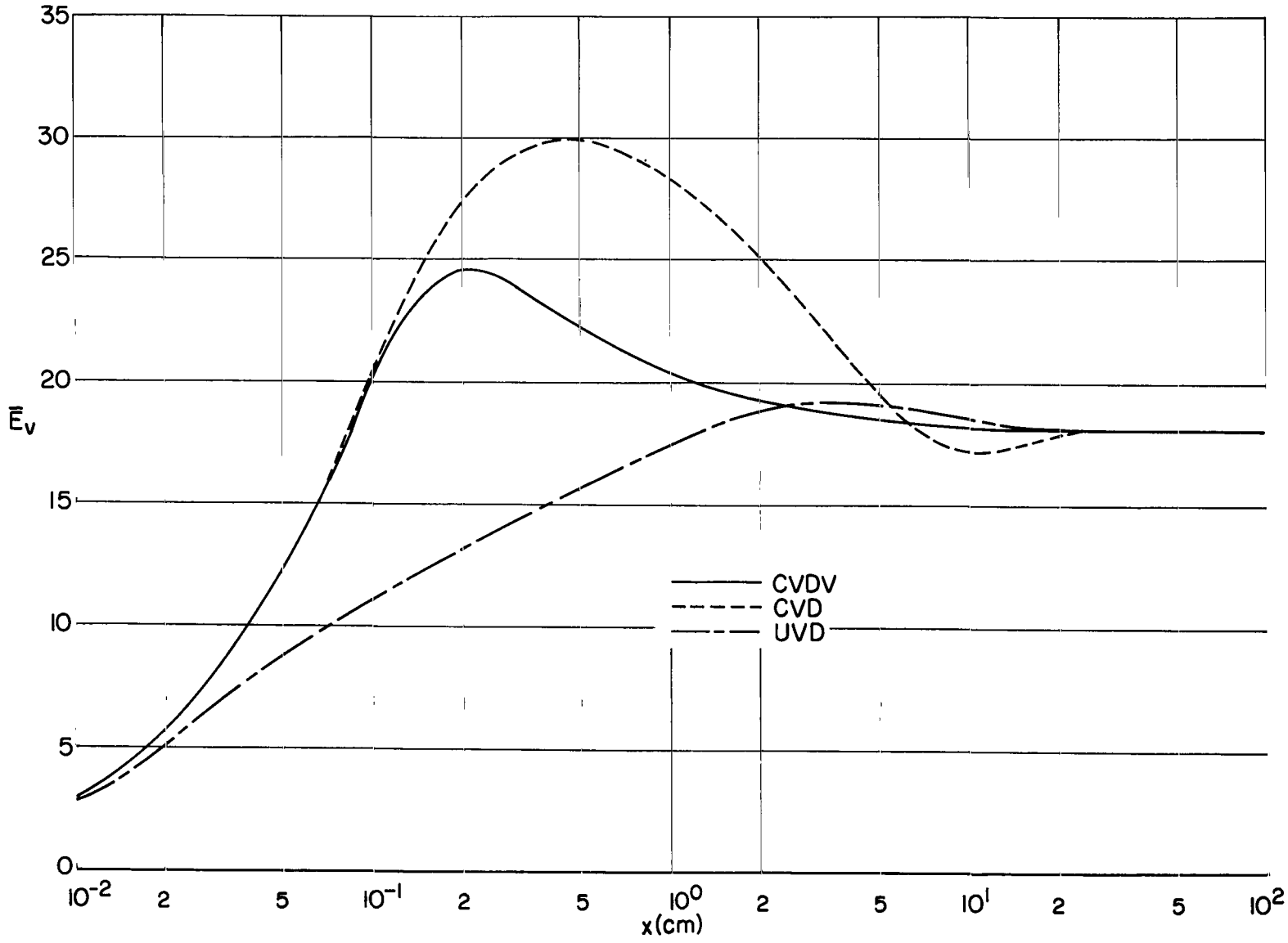

Figure 7.- Vibrational energy along wedge surface for Case II.

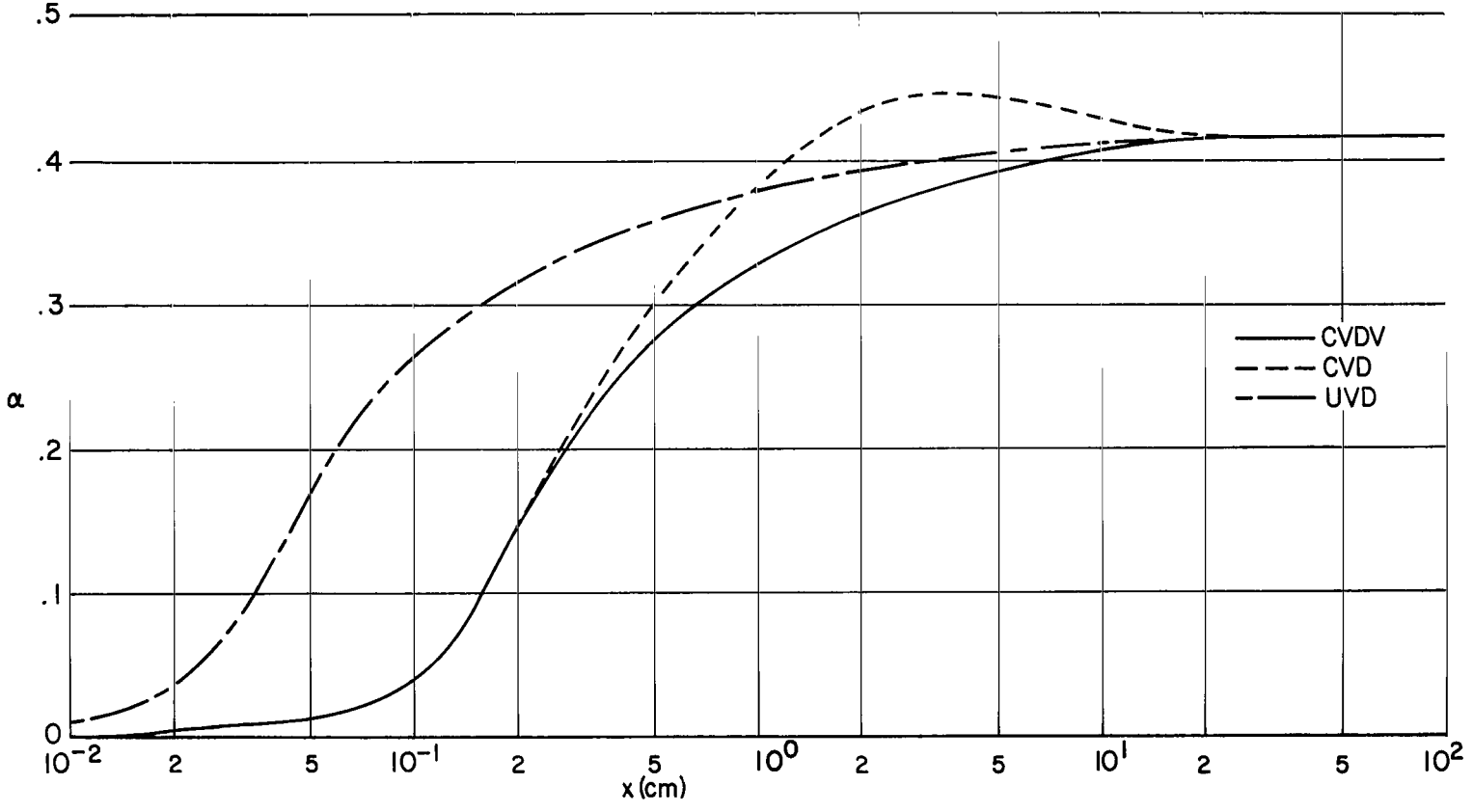

Figure 8.- Atom mass fraction along wedge surface for Case II.

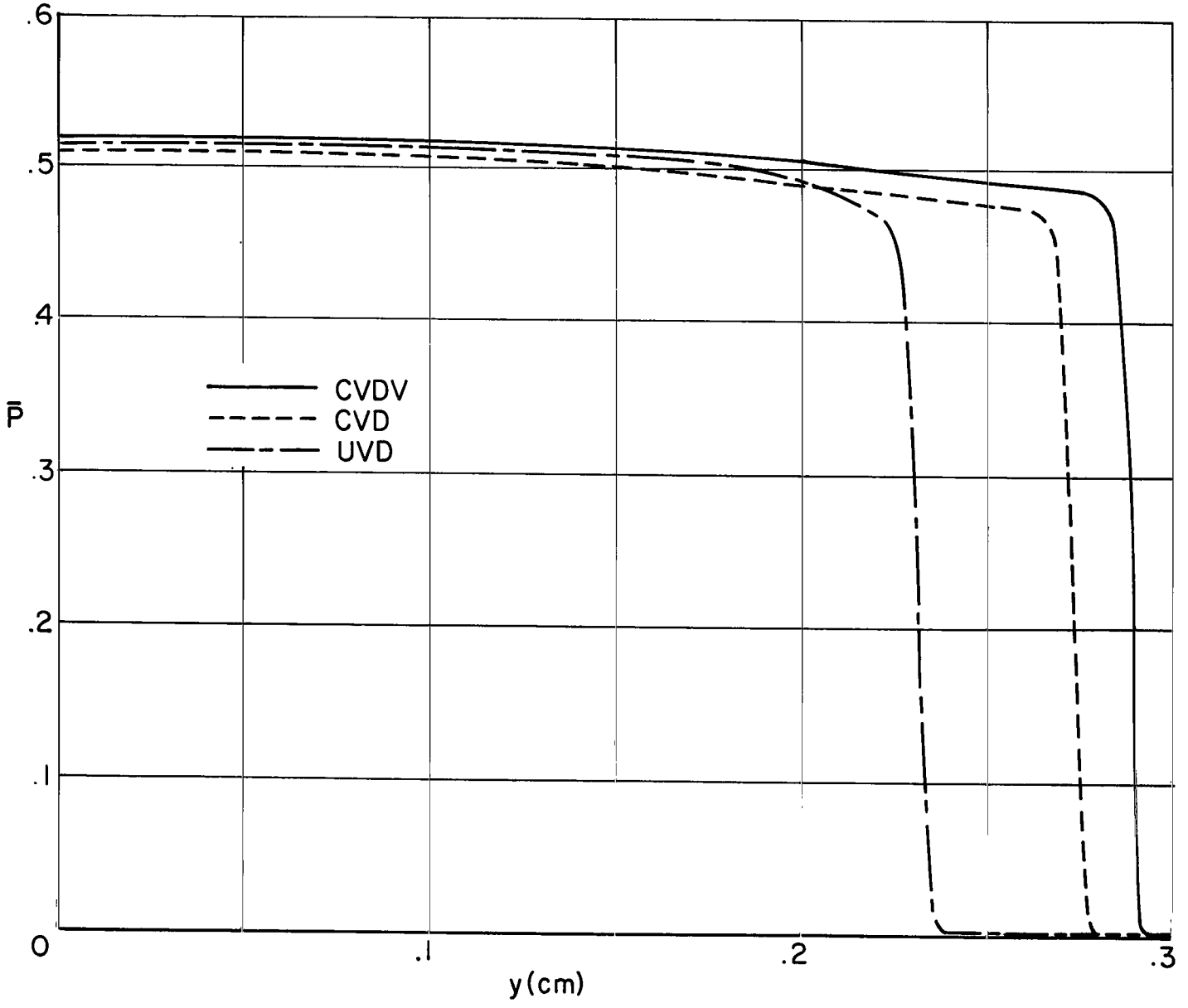

Figure 9.- Pressure profile normal to wedge surface at x = 2 cm for Case II.

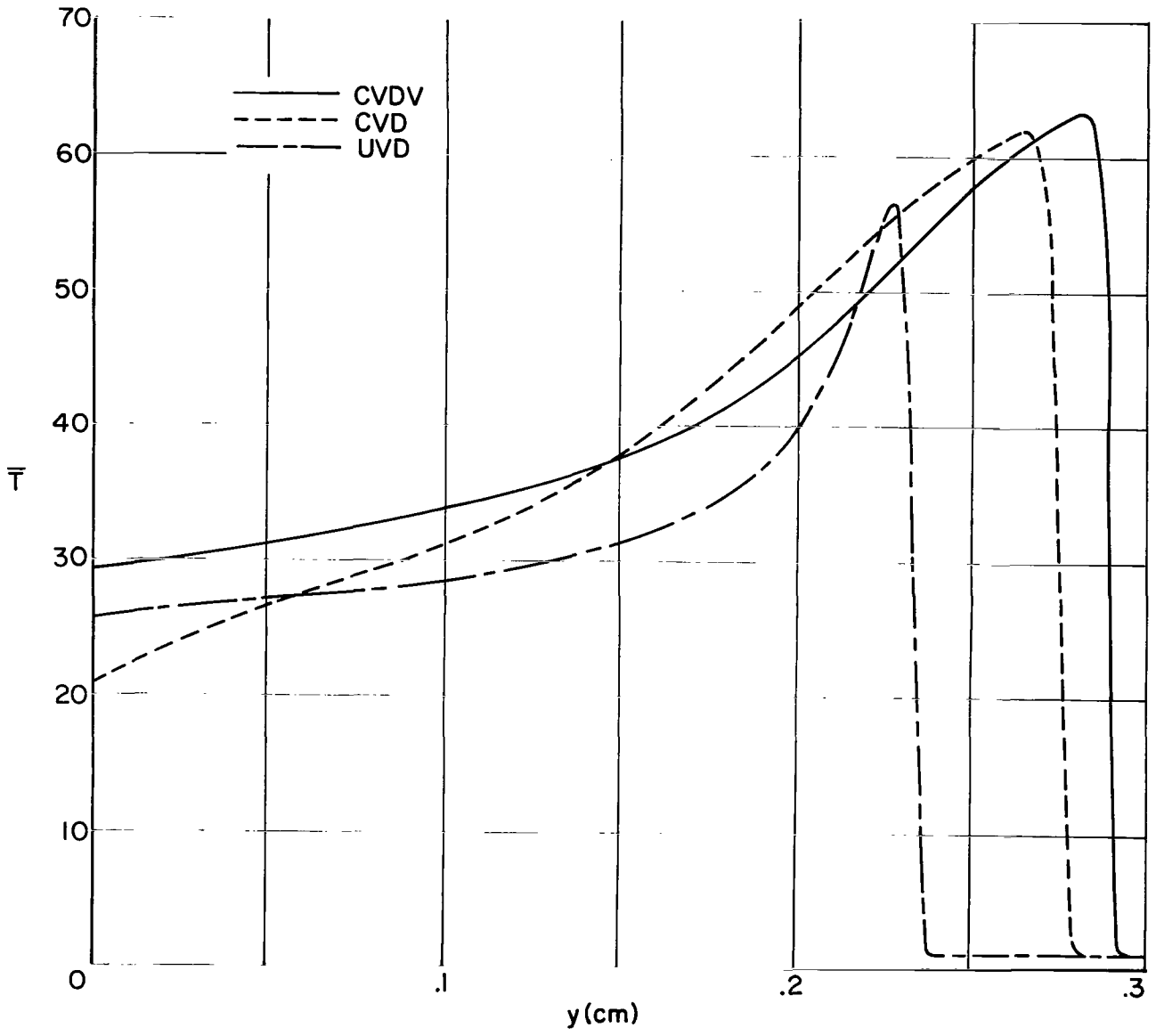

Figure 10.- Temperature profile normal to wedge surface at x = 2 cm for Case II.

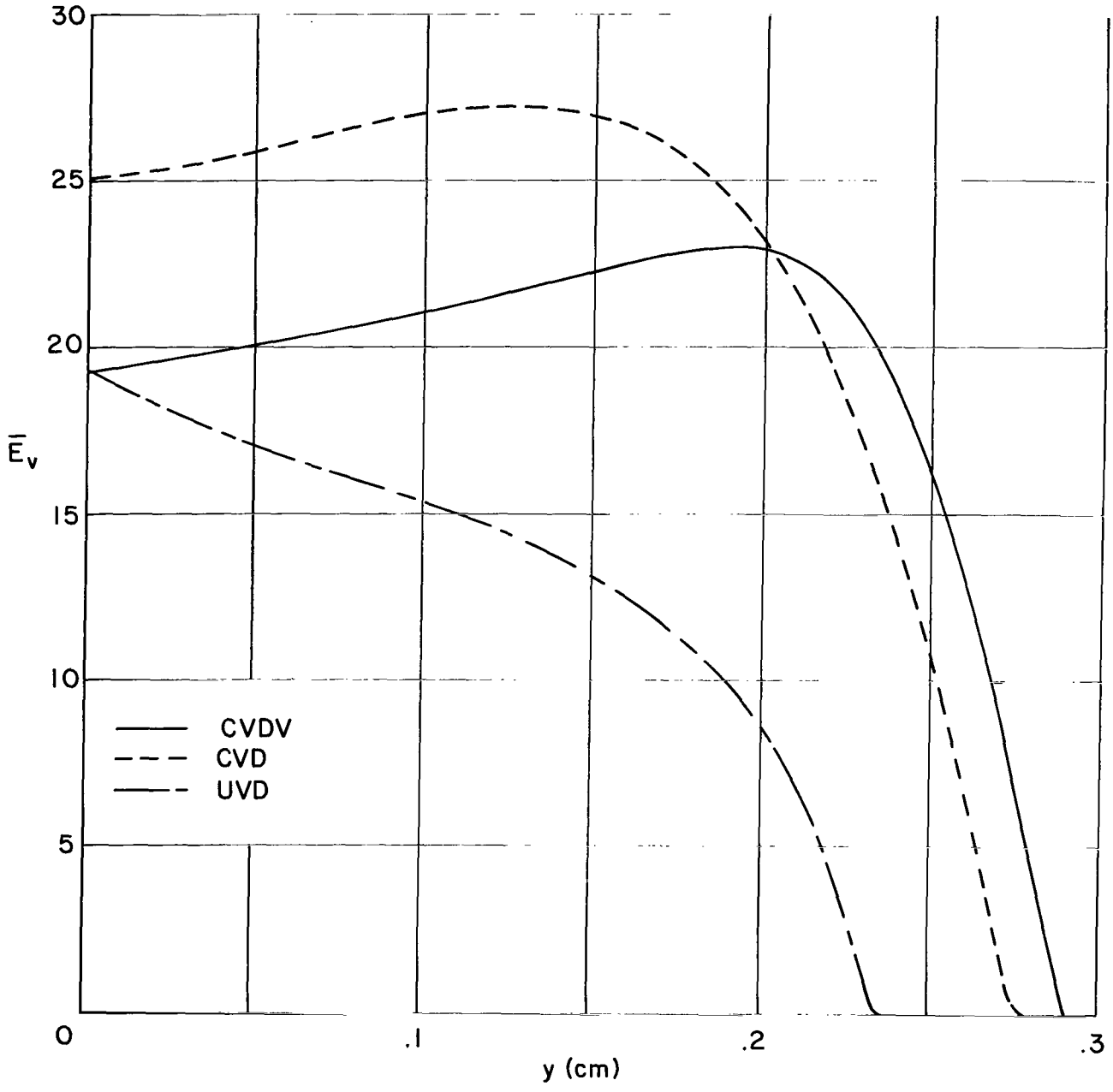

Figure 11.- Vibrational energy profile normal to wedge surface at x = 2 cm for Case 11.

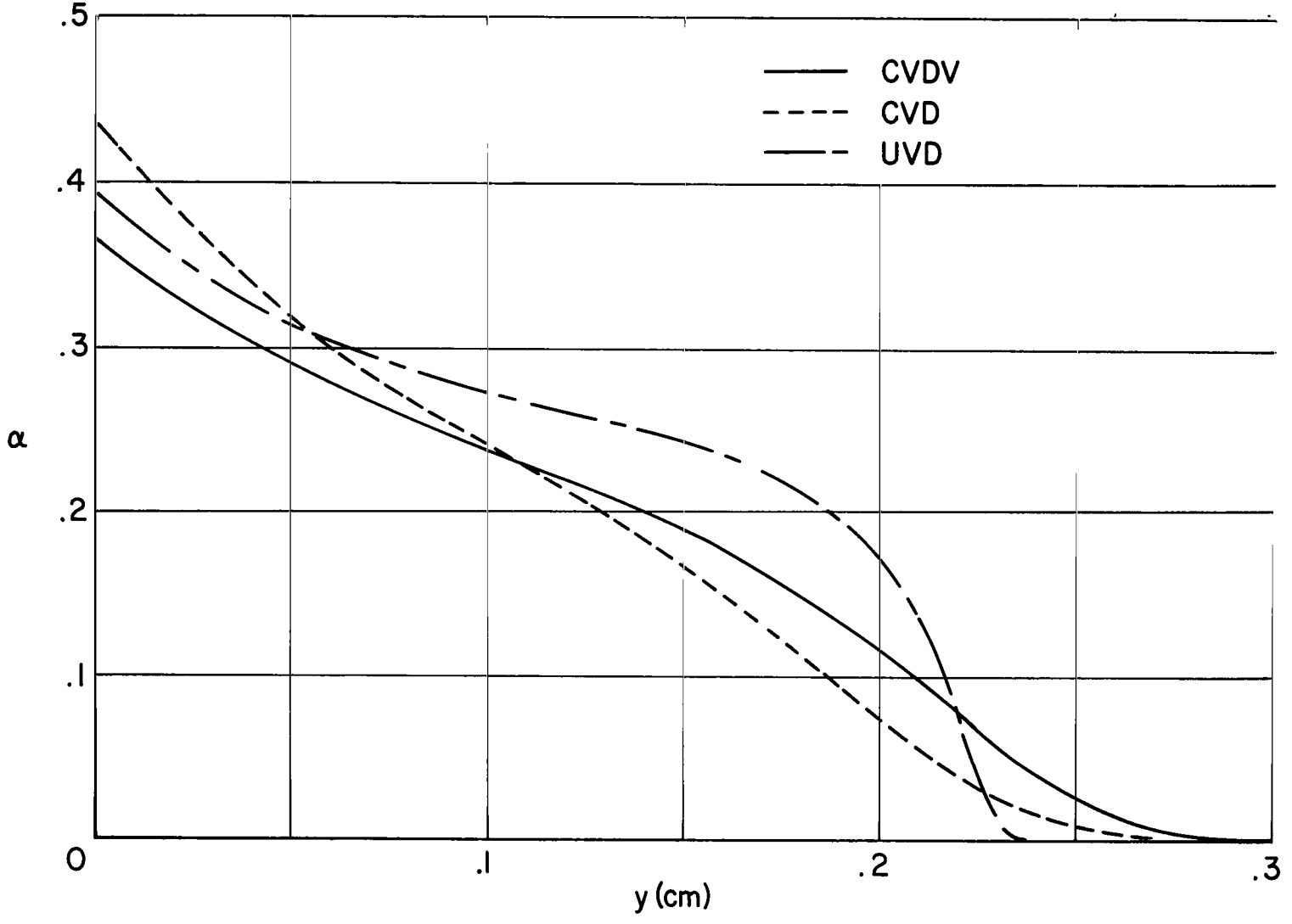

Figure 12.- Atom mass-fraction profile normal to wedge surface at x = 2 cm for Case 11.

"The aeronautical and space activities of the United States shall be conducted so as to contribute . . . to the expansion of human knowledge of phenomena in the atmosphere and space. The Administration shall provide for the widest practicable and appropriate dissemination of information concerning its activities and the results thereof."

—NATIONAL AERONAUTICS AND SPACE ACT OF 1958

NASA SCIENTIFIC AND TECHNICAL PUBLICATIONS

TECHNICAL REPORTS: Scientific and technical information considered important, complete, and a lasting contribution to existing knowledge.

TECHNICAL NOTES: Information less broad in scope but nevertheless of importance as a contribution to existing knowledge.

TECHNICAL MEMORANDUMS: Information receiving limited distribution because of preliminary data, security classification, or other reasons.

CONTRACTOR REPORTS: Technical information generated in connection with a NASA contract or grant and released under NASA auspices.

TECHNICAL TRANSLATIONS: Information published in a foreign language considered to merit NASA distribution in English.

TECHNICAL REPRINTS: Information derived from NASA activities and initially published in the form of journal articles.

SPECIAL PUBLICATIONS: Information derived from or of value to NASA activities but not necessarily reporting the results of individual NASA-programmed scientific efforts. Publications include conference proceedings, monographs, data compilations, handbooks, sourcebooks, and special bibliographies.

Details on the availability of these publications may be obtained from:

SCIENTIFIC AND TECHNICAL INFORMATION DIVISION

NATIONAL AERONAUTICS AND SPACE ADMINISTRATION

Washington, D.C. 20546